

Accepted refereed manuscript of:

Lamprianidou F, Telfer T & Ross L (2015) A model for optimization of the productivity and bioremediation efficiency of marine integrated multitrophic aquaculture, *Estuarine, Coastal and Shelf Science*, 164, pp. 253-264.

DOI: [10.1016/j.ecss.2015.07.045](https://doi.org/10.1016/j.ecss.2015.07.045)

© 2015, Elsevier. Licensed under the Creative Commons Attribution-NonCommercial-NoDerivatives 4.0 International
<http://creativecommons.org/licenses/by-nc-nd/4.0/>

1 A MODEL FOR OPTIMIZATION OF THE PRODUCTIVITY AND BIOREMEDIATION
2 EFFICIENCY OF MARINE INTEGRATED MULTITROPHIC AQUACULTURE

3
4 Fani Lamprianidou*, Trevor Telfer and Lindsay G. Ross

5
6 Institute of Aquaculture, University of Stirling, Stirling FK9 4LA, UK

7 *Corresponding author. E-mail address: fani.lamprianidou@stir.ac.uk

8
9 *Keywords: IMTA, Ulva, Paracentrotus lividus, Dynamic energy budget, Nitrogen, modelling*

10
11 Abstract

12 Integrated multitrophic aquaculture (IMTA) has been proposed as a solution to
13 nutrient enrichment generated by intensive fish mariculture. In order to evaluate the potential
14 of IMTA as a nutrient bioremediation method it is essential to know the ratio of fed to
15 extractive organisms required for the removal of a given proportion of the waste nutrients.
16 This ratio depends on the species that compose the IMTA system, on the environmental
17 conditions and on production practices at a target site. Due to the complexity of IMTA the
18 development of a model is essential for designing efficient IMTA systems. In this study, a
19 generic nutrient flux model for IMTA was developed and used to assess the potential of
20 IMTA as a method for nutrient bioremediation. A baseline simulation consisting of three
21 growth models for Atlantic salmon *Salmo salar*, the sea urchin *Paracentrotus lividus* and for
22 the macroalgae *Ulva* sp. is described. The three growth models interact with each other and
23 with their surrounding environment and they are all linked via processes that affect the release
24 and assimilation of particulate organic nitrogen (PON) and dissolved inorganic nitrogen
25 (DIN). The model's forcing functions are environmental parameters with temporal variations,
26 which enables investigation of the understanding of interactions among IMTA components
27 and of the effect of environmental parameters. The baseline simulation has been developed
28 for marine species in a virtually closed system in which hydrodynamic influences on the
29 system are not considered. The model can be used as a predictive tool for comparing the
30 nitrogen bioremediation efficiency of IMTA systems under different environmental
31 conditions (temperature, irradiance and ambient nutrient concentration) and production
32 practices, for example seaweed harvesting frequency, seaweed culture depth, nitrogen content
33 of feed and others, or of IMTA systems with varying combinations of cultured species
34 (salmon, seaweed, sea urchins) and can be extended to open water IMTA once coupled with
35 waste distribution models.

36

37 1. Introduction

38 The constantly increasing demand for seafood, during a period of overexploitation of the
39 fisheries sector can only be met by sustainable growth of aquaculture. This growth is limited
40 by the environmental impacts and economic requirements of intensive monoculture of fed
41 species. Moreover, rapid and uncontrolled expansion of the aquaculture sector challenges the
42 realization of an Ecosystem Approach to Aquaculture (Soto, 2008). If industry expansion is
43 not regulated and developed appropriately, it has the potential to cause further damage to the
44 environment. It has been proposed that expansion of marine aquaculture in parallel with
45 environmental protection can be achieved using Integrated Multi-Trophic Aquaculture
46 systems (IMTA) (Chopin et al. 2001; Neori et al. 2004). IMTA has the potential to be an
47 economically viable solution to the problems of dissolved and particulate nutrient enrichment,
48 since the waste from fed species aquaculture is exploited as a food source by extractive
49 organisms of lower trophic levels giving added value to the investment in feed by producing a
50 low input protein source as well as increasing the farm income. For example, in order to
51 promote more resilient growth of the aquaculture industry in Scotland, a draft Seaweed Policy
52 Statement that examines the cultivation of seaweed in general, and as part of IMTA systems
53 was introduced in 2013 (Marine Scotland, 2013). Large-scale seaweed cultivation has been
54 suggested as a means to mitigate the nutrient enrichment environmental impact of marine fish
55 farms (Abreu et al. 2009; Fei et al. 1998; Wang et al. 2013). As a very large area is required
56 for the cultivation of sufficient seaweed biomass for complete nutrient bioremediation, doubt
57 remains as to whether complete bioremediation by seaweed cultivation is practically feasible
58 (Broch and Slagstad, 2012). However, there is a general agreement that cultivation of
59 seaweed as part of an IMTA is a promising way for partial removal of dissolved fish farm
60 effluent (Broch et al. 2013; Jiang et al. 2010; Reid 2013; Wang et al. 2013). The amount of
61 excess nutrients released from sea cages depends on the fish species and on farm practises. In
62 salmon monoculture, approximately 62% of the nitrogen (N) and 70% of the phosphorus (P)
63 input from feed is lost to the environment as feed wastage (non-consumed food) and fish
64 excretory waste products (Wang et al. 2012). Particulate waste derived from intensive fed
65 aquaculture is deposited in the proximity of sea cages and can lead to changes in sediment
66 chemistry, oxygen availability and in the number and diversity of benthic species (Corner et
67 al. 2006).

68

69 From a biological point of view, the choice of extractive species in an IMTA system is crucial
70 because their physiology and their ecological attributes determine the rate of particle or
71 nutrient consumption and assimilation, their growth rate and in capabilities in terms of
72 biofiltration. Species are chosen based on specific culture performance traits, for which

73 quantitative information needs to be available, with respect to nutrient uptake efficiency and
74 secondary considerations (e.g. yield and protein content). The marketability of the extractive
75 species is largely dependent on the location, with the Western world showing less demand for
76 food species that are low in the trophic chain. Nevertheless, dried seaweed products can
77 always be exported and seaweeds can be processed to produce cosmetics, fertilizers, animal
78 feed, biogas and others.

79

80 The environmental benefits, matter and energy flux within an IMTA farm as well as between
81 the environment and the IMTA system, need to be qualified and quantified prior to the
82 establishment of a marine IMTA system. The aim of this study was to provide a tool for
83 designing IMTA farms at any site by creating a modelling tool that can be used to fine-tune
84 IMTA designs for maximising yields and nutrient removal.

85

86 Without a thorough understanding of the system's dynamic, the environmental and
87 economical benefits of IMTA cannot be achieved. However, field measurements of nutrient
88 and Particulate Organic Matter (POM) concentrations in open-water systems are challenging
89 due to the highly diluting, dynamic nature of open-water systems, presenting high spatial and
90 temporal variation both diurnally and seasonally. The model described in this study
91 determines the temporal availability of nutrients and POM released by the different IMTA
92 components and thus the amount available for uptake by different groups of extractive
93 organisms. Because of the site specificity of waste distribution, this model focuses on
94 simulation of a virtually closed system, within which the nitrogen is homogeneously
95 distributed. The species used in this study are Atlantic salmon (*Salmon salar*), a sea urchin
96 (*Paracentrotus lividus*) and the sea lettuce (*Ulva lactuca*), though it will be possible to re-
97 parameterise for a range of different species.

98

99 2. Model development

100

101 The model was implemented using the visual simulation package Powersim™ Constructor
102 Studio 8 (Powersim Software AS, Bergen), which supports structural construction, equation
103 deduction and computer implementation of a conceptual model. The time horizon used was
104 an 18-month period, to simulate the at-sea phase of salmon production cycle, which can last
105 between 14 and 24 months (Marine Harvest, 2012). The model is typically operated with a
106 one day time step and the model's differential equations were solved using a third order
107 Runge-Kutta integration method. The selected time-step can reflect accurately all the

108 important time dependent environmental changes (accurate integration) with low computing
109 effort.

110

111 An extensive literature review was carried out for model parameterization for *Ulva* (see Table
112 1) and for *Paracentrotus lividus* (Add_my_pet, 2014), while the model for *Salmo salar* was
113 parameterized using data acquired from commercial Scottish salmon farms. For some
114 parameters, a range of values was available in the literature in which case the most
115 representative value was used. It is evident that the inclusion of many proxy variables from
116 the literature propagates uncertainties through the model, which affects the overall model
117 accuracy. Since the model presented in this study is deterministic, its output is entirely
118 determined by the input parameters and structure of the model. Due to the high structural
119 complexity of the model and high degree of uncertainty in estimating the values of many
120 input parameters, a detailed sensitivity analysis was performed by varying each input
121 parameter by $\pm 10\%$ and quantifying the effect on eight output variables (Tables 3-6). The
122 selected output variables reflect the objectives of the research with respect to nitrogen
123 bioremediation and yield productivity. Within the sensitivity analysis all model parameters
124 and initial values of state variables (50 input variables) were varied in order to determine the
125 response of the following eight effect variables: harvested biomass of seaweed, salmon and
126 sea urchin, nitrogen accumulated by the seaweed, salmon and sea urchin, DIN and PON
127 available at the IMTA site at the end of the simulation. The sensitivity analysis results are
128 presented as a normalized sensitivity coefficient (NS) (Fasham et al. 1990):

129

$$130 \quad NS = \frac{DV/V_b}{DP/P_b} \quad (1)$$

131

132 where, $DV = (V_b - V)$ is the change of a response variable, V_b is the value of a response
133 variable for the base run, V is the value of a response variable for the sensitivity analysis run,
134 $DP = (P_b - P)$ is the change in a model parameter, P_b is the baseline value of a model
135 parameter and P is the value of a model parameter for the sensitivity analysis run.

136

137 When the value of NS for a parameter +10% is negative then there is a negative correlation
138 between parameter and effect. When it is negative for a parameter -10% then there is a
139 positive correlation between parameter and effect.

140

141 2.1 Model outline

142

143 The model determines the nutrient recovery efficiency and biomass production of IMTA
144 systems based on a baseline simulation so that components of the model can be altered or
145 removed for the simulation of particular scenarios. Following re-parameterization, the model
146 can simulate IMTA systems consisting of different finfish, sea urchin (or other grazing
147 invertebrate) or seaweed combinations of species. The present model is for an IMTA system
148 comprising of Atlantic salmon (*Salmo salar*), seaweed (*Ulva* sp.) and sea urchins
149 (*Paracentrotus lividus*). It incorporates an ecosystem model consisting of three submodels
150 that interact with each other and with their surrounding environment via nutrient cycling (Fig.
151 1). The submodels consist of growth models for salmon, seaweed and sea urchin that include
152 nitrogen uptake and release via feed intake and excretion, and interact with each other through
153 modelled nitrogen release and subsequent assimilation (Fig. 1).

154

155 Insert fig. 1 here

156

157 Salmon growth was modelled using the Thermal-unit Growth Coefficient (TGC) (Iwama and
158 Tautz, 1981), the seaweed growth model is based on Droop's model for nutrient-limited algal
159 growth (Droop, 1968) and sea urchin growth was modeled using the Dynamic Energy Budget
160 (DEB) theory (Kooijman 1986). In principle, all three models are DEB models because the
161 TGC is a special case of the Von Bertalanffy equation (Dumas et al. 2010) which, along with
162 Droop's model for nutrient-limited algal growth (Kooijman, 2008), is a special case of the
163 DEB approach.

164

165 The TGC is a simple model widely used in aquaculture, based on three basic assumptions,
166 which may be violated under certain conditions (Jobling, 2003). Firstly, growth rate increases
167 linearly with temperature, secondly the length (L) and weight (W) relationship is $W \propto L^3$, and
168 thirdly the growth in length for any given temperature is constant over time (Jobling, 2003).
169 The TGC can present errors when the temperature deviates far from the optimum for growth
170 (Jobling 2003), but this is not a setback given the temperature range used in the present
171 simulations. For the organic extractive organisms a bioenergetic model was used in order to
172 link the environmental variables, mainly food availability and temperature, with feed intake,
173 growth, excretion and faeces production. For the simulation of salmon growth and nutrient
174 uptake and release, the TGC was preferred to a bioenergetic model because under intensive
175 aquaculture conditions feed is not limiting growth. Furthermore, salmon is well studied and
176 daily time series data for the TGC and food conversion ratio (FCR) as well as sources of data
177 for excretions and faeces production were available in the literature. Finally, as salmon are

178 grown at sea for only for a part of their production, data are not required for the full life cycle,
179 which is the strength of the DEB approach.

180

181 The model includes daily time steps for better understanding of the process affecting the
182 IMTA productivity and nutrient removal efficiency. Due to the dynamic design of the model
183 the bioremediation potential of different production scenarios can be estimated by altering
184 various production parameters of the baseline simulation. These include site-specific
185 environmental conditions (temperature, irradiance and ambient nutrient concentration) and
186 production practices (seaweed harvesting frequency, seaweed culture depth, nitrogen content
187 of feed, initial stocking biomass of extractive organisms etc.). The maximum seaweed and sea
188 urchin biomass that can be sustained at any given time can also be estimated based on the
189 daily amount of nitrogen within the IMTA system that is available for uptake.

190

191 The complete model is used to determine the overall ability of the IMTA system to reduce the
192 nutrient and POM waste of fed-species monoculture taking into account the quantity of
193 nutrients and POM that are released and the quantity that could be potentially
194 absorbed/consumed by the extractive organisms if all the waste remained within the virtually
195 closed system. The only nitrogenous input to the seaweed and sea urchin submodels is the
196 daily waste released to the sea from the salmon submodel. This is used to calculate the
197 amount of particulate (suspended) and dissolved nitrogen released from the salmon farm for a
198 given fish production over 18 months, as well as the potential for decreasing the nutrient
199 released by converting salmon monocultures into IMTA systems. The model takes into
200 account fish growth and consequent feed input and waste release, and the uptake and release
201 of DIN and PON by the different IMTA components. The growth models are combined with
202 nutrient transfer/cycling and this way the virtually closed system bioremediation efficiency is
203 estimated (Fig. 1).

204

205 2.2 Salmon growth submodel

206 The growth rate of fish fluctuates throughout an individual's life cycle and is mainly
207 influenced by feed availability, temperature and photoperiod (Austreng et al. 1987; Brett,
208 1979). Salmon growth was simulated using a thermal growth coefficient:

209

$$210 \quad TGC = 1000 \frac{\sqrt[3]{W_t} - \sqrt[3]{W_0}}{T * t} \quad (2)$$

211

212 where, TGC is the thermal growth coefficient, W_0 is the initial wet weight of the smolt, W_t is
213 the wet weight of the fish at time t , T is the temperature and t is time in degree-days.

214 Solving for W_t we obtain:

215

$$216 \quad W_t = \left[\sqrt[3]{W_0} + \frac{TGC * T * t}{1000} \right]^3 \quad (3)$$

217

218 The total salmon biomass was calculated as individual weight multiplied by the number of
219 individuals. The model also accounted for natural mortality, modeled as a time series variable
220 since mortality decreases with fish size, using empirical data from Scottish salmon farms.

221

222 The amount of waste released from the salmon farm in the form of excretion, faeces
223 production and feed loss was assumed to be as calculated by Wang et al (2012) for
224 Norwegian salmon farms. In detail, we assume that every day of the simulation 2% of the
225 feed nitrogen is released in the environment in the form of feed loss, 45% in the form of
226 dissolved excretions and 15% in the form of faeces, while the remaining 38% is assimilated
227 into the salmon biomass and removed from the ecosystem when the fish are harvested. The
228 nitrogen content of the feed was set to be 7.2% of the feed weight (Gillibrand et al. 2002).

229

230 2.3 Seaweed growth and nitrogen uptake

231

232 Seaweed biomass (B) increases with a varying growth rate and decreases due to both natural
233 causes and periodic harvesting. The basic processes affecting seaweed biomass form the
234 differential equation 4:

235

$$236 \quad \frac{dB}{dt} = (\mu - \Omega) * B - (D + H) * B \quad (4)$$

237 where, μ is the specific growth rate, Ω the specific decomposition rate, D the loss rate due to
238 environmental disturbance and H the harvesting rate. Biomass is calculated as wet biomass,
239 for the conversion of seaweed wet to dry weight an 8.43 to 1 ratio was used (Angell et al.
240 2012; Neori et al. 1991). At the baseline simulation due to lack of data in the literature for the
241 specific decomposition rate and the loss due to environmental disturbance for *Ulva* sp. the
242 term mortality (M) is used, where $M = \Omega + D$ and $\Omega = D$ (Table 1).

243

244 The gross growth rate was defined as a function of water temperature, availability of
245 Photosynthetic Active Radiation (PAR) and nutrient concentration in the water column and in
246 the plant tissues. The joint dependence of growth on environmental variables is defined by
247 separate growth limiting factors, which can range between 0 and 1. A value of 1 means the
248 factor does not inhibit growth (i.e. light is at optimum intensity, temperature is optimum and

249 nutrients are available in excess). The limiting factors are then combined with the maximum
 250 gross growth rate at a reference temperature as in equation 5 (Solidoro et al. 1997):

251

$$252 \quad \mu = \mu_{\max(T_{ref})} * f(T) * f(I) * \min(f(N), f(P)) \quad (5)$$

253

254 where, $\mu_{\max(T_{ref})}$ is the maximum growth rate at a particular reference temperature (T_{ref}) under
 255 conditions of saturated light intensity and excess nutrients, $f(T), f(I), f(N), f(P)$ are the growth
 256 limiting functions for temperature, light and nutrients (nitrogen and phosphorus).

257

258 The major nutrients required for growth are nitrogen and phosphorus, while carbon is often
 259 available in excess and micronutrients such as iron and manganese are only limiting in
 260 oligotrophic environments. Typically, in marine ecosystems, nitrogen is the element limiting
 261 algal growth (Lobban and Harrison, 1994). Thus in the baseline simulation it is assumed that
 262 phosphorus is not limiting, so Eq. 5 becomes:

263

$$264 \quad \mu = \mu_{\max(T_{ref})} * f(T) * f(I) * f(N) \quad (6)$$

265

266 The Photosynthetic response to light is based on Steele's photoinhibition law (Steele, 1962):

267

$$268 \quad \frac{P}{P_{\max}} = \frac{I}{I_{opt}} \exp \frac{1-I}{I_{opt}} \quad (7)$$

269

270 where, P is the photosynthetic response at a given light intensity I (W m^{-2}) for an organism
 271 that has a maximum photosynthetic rate P_{\max} at the optimal (saturating) light intensity I_{opt} and
 272 I is the light intensity at a given depth (z). Light intensity at a given depth is an exponential
 273 function of depth, seaweed and phytoplankton standing biomass and is given by:

$$274 \quad I(z) = I_0 e^{-kz} \quad (8)$$

275

276 After mathematical integration of the light limitation factor Eq. 8 we obtain:

277

$$278 \quad F(I) = \int_0^z \frac{P}{P_{\max}} dz = \int_0^z \frac{I(x)}{I_{opt}} \exp \frac{1-I(x)}{I_{opt}} dx = \int_0^z \frac{I_0 e^{-kx}}{I_{opt}} \exp \frac{1-I_0 e^{-kx}}{I_{opt}} dx = \frac{1}{k} * \exp \left(\frac{1}{I_{opt}} \right) * \\ 279 \quad \left[\exp \left(-\frac{I_0}{I_{opt}} * \exp(-z * k) \right) - \exp \left(-\frac{I_0}{I_{opt}} \right) \right] \quad (9)$$

280 where, k is the light extinction coefficient (m^{-1}), z is the culture depth (m), I_{opt} is the optimal
 281 light intensity and P is the photosynthetic rate at a given light intensity I (W m^{-2}).

282

283 The temperature, like the light, limitation factor follows an inhibition law.

284

$$285 \quad F(T) = q_{10}^{0.1(T-T_{ref})} \quad (10)$$

286

287 where, q_{10} is a temperature coefficient, T is the water temperature and T_{ref} is the reference
288 temperature at which the seaweed growth rate was measured. The q_{10} temperature coefficient
289 is a measure of the rate of change of a biological or chemical system as a consequence of
290 increasing the temperature by 10°C (Raven and Geider, 1988).

291

292 The nitrogen limitation factor Eq. 11 is given by the range of internal nitrogen concentration,
293 with a feedback effect on the uptake function (Aveytua-Alcázar et al. 2008; Coffaro and
294 Sfriso, 1997; Solidoro et al. 1997; Trancoso et al. 2005; Zaldívar et al. 2009). It can range
295 between 1, when $N = N_{max}$ and uptake is saturated and 0 when $N = N_{min}$ and maximum uptake
296 rate is possible, all measured in mg N per g dry seaweed. Internal nitrogen
297 quota/concentration (N) refers to the concentrations in the algal cells as opposed to external
298 concentrations that refers to the concentration amount in the water column.

299

$$300 \quad F(N) = 1 - \frac{N_{max} - N}{N_{max} - N_{min}} \quad (11)$$

301

302 where, N_{max} is the maximum internal quota of nitrogen and N_{min} the minimum.

303

304 For calculation of the nitrogen quota (N), a quota-based model was used developed from
305 Droop's original formula (Droop, 1968):

306

$$307 \quad \frac{dN}{dt} = V * F(N) - \mu * N \quad (12)$$

308

309 where, V is the nitrogen uptake rate ($\text{mg g}^{-1}\text{dw h}^{-1}$) and μ is the specific growth rate.

310

311 Nutrient uptake rates (V) are proportional to nutrient concentration in the water column
312 according to Michaelis–Menten kinetics:

313

$$314 \quad V = \frac{V_{max}S}{K_N+S} \quad (13)$$

315

316 where, V_{max} is the maximum nitrogen uptake rate under the prevailing conditions at the site
 317 ($\text{mg g}^{-1}\text{dw h}^{-1}$), S is the total DIN concentration in the seawater (mg l^{-1}) and K_N is the half-
 318 saturation coefficient for the uptake of nitrogen (mg l^{-1}).

319

320 By combining Eqs. 11, 12 and 13 we obtain:

321

$$322 \quad \frac{dN}{dt} = \frac{V_{max} S}{K_N + S} \frac{N_{max} - N}{N_{max} - N_{min}} - (\mu * N) \quad (14)$$

323

324 The bioremediation effect of IMTA is closely dependent on the biomass of extractive
 325 organisms harvested. However, the maximum biomass is restricted by culture practicalities
 326 such as the potential alteration of water currents and by the availability of nutrients. The
 327 maximum biomass is site and species dependent, and for the baseline simulation presented in
 328 this study the maximum seaweed biomass permitted to be on site at any given time was set at
 329 35 tonnes wet weight. The area required for the culture of 35 t of *Ulva*, with stocking density
 330 of 1.6 kg/m^2 and two layers of seaweed one at the sea surface and one 3 m deep would be
 331 $10,937 \text{ m}^2$. This stocking density was selected because the maximum density permitted to
 332 guarantee the greatest uptake of nutrients in *U. lactuca* is 1.9 kg m^{-2} (Neori et al. 1991). The
 333 area required for the seaweed culture is used for the estimation of the virtually closed IMTA
 334 site's water volume, which is estimated using the following formula:

335

336 'IMTA site volume' = 'Average depth' * 'Number of salmon cages' * 'Sea cage area' + 'raft
 337 area' * 'number of rafts' * 'Average depth'.

338

339 Seaweed is lost due to mortality, harvesting and natural biomass loss (seedling mortality,
 340 grazing, epiphytism, sediment abrasion and smothering and removal by wave action).
 341 Managing the harvesting rate is of paramount importance for achieving high productivity
 342 rates. For optimal results, in the present model, when the seaweed biomass reaches a
 343 predefined level (35 t in the baseline simulation) the seaweed is harvested at regular time
 344 intervals. The biomass harvested depends on the forecasted growth and natural mortality rate
 345 of the forthcoming days. A discrete flow in the model controls the loss of seaweed biomass
 346 due to harvesting; the rate of the flow (harvest rate) is regulated by the following instruction:

347

348 *IF* (start harvesting = 0, 0 ton, *IF* (current time step * timestep = stoptime - starttime,
 349 seaweed biomass, *IF* (accrued part of 10 days = 1, seaweed biomass – maximum seaweed
 350 biomass, *IF* (accrued part of 10 days = 0, seaweed biomass – maximum seaweed biomass, 0
 351 ton))))

352

353 where, 'start harvesting' is a level that allows harvesting to start only when the seaweed
354 biomass has surpassed the value of a constant that defined as maximum biomass that can be
355 on site (maximum seaweed biomass). The level 'start harvesting' changes from 0 to 1 when
356 the level 'seaweed biomass' is equal to or larger than the constant 'maximum seaweed
357 biomass'. 'Current time step' is a level that counts the time steps, starting from zero. *Timestep*
358 is a Powersim built-in function that returns the time step of the simulation, *starttime* and
359 *stoptime* are Powersim built-in functions that return the start-time and stop-time of the
360 simulation, respectively. In the final time step all the seaweed in the level 'seaweed biomass'
361 is transferred to the level 'harvested seaweed'. 'Seaweed biomass' is a level that shows the
362 seaweed biomass. 'Accrued part of 10 days' is a level used for the calculation of 10-day
363 periods. When the value of this level is one, all the seaweed is harvested apart from
364 'maximum seaweed biomass'.

365

366 The model is effective for perennial seaweed species. However, as the gametophyte stage of
367 *Ulva*, lasts only for a few months, frequent reseeding will be necessary at time intervals
368 dependent on the environmental conditions, epiphytic growth or disease. The numerical
369 parameters used in the seaweed model are summarized in Table 1.

370

371 Insert Table 1 here

372

373 2.4 Sea urchin growth and nitrogen uptake and release

374

375 The sea urchin growth submodel is based on the Dynamic Energy Budget (DEB) theory
376 (Kooijman, 1986). A DEB model describes and interconnects the physiological processes that
377 occur within an individual as a function of the state of the individual and the environment
378 (Kooijman, 2001). DEB theory is based on two state variables: structural volume (V) and
379 energy reserves (E) and on two forcing variables: temperature (T) and food density (X). The
380 basic concept of the theory is that from the food ingested a certain amount is released as
381 faeces and the rest is assimilated. All the assimilated food enters a reserve compartment.
382 From there a fixed fraction will be spent on maintenance and the rest will spend on maturity
383 or reproduction (Kooijman, 1986). A detailed description of the DEB can be found at
384 Kooijman (2008). Most of the species-specific parameters used for this DEB model were
385 obtained from (Kooijmann, 2014).

386

387 The initial structural length/diameter of the sea urchin juveniles was set to 10 mm, because at
 388 this size hatchery reared sea urchins can be transferred to sea successfully (Kelly et al. 1998).
 389 At this length *P. lividus* individuals are characterized as sub adults (Grosjean et al. 1998), so
 390 in the baseline simulation the DEB model simulates the growth from late juveniles to mature
 391 adults. The physical length (L_w) was converted to volumetric length (L):

$$392$$

$$393 L_w = L / \delta_M \quad (15)$$

394
 395 where, δ_M is the shape coefficient.

396
 397 For this simulation the notation from Kooijman (2000) was used. All rate variables are dotted
 398 above, all variables that are expressed per unit volume and per unit surface area are given
 399 between square brackets and braces, respectively. Additionally, the expression (x)+ is defined
 400 as: $[x]^+ = x$ for $x > 0$, $[x]^+ = 0$.

401 Most of the processes described by the DEB model are influenced by the effect of
 402 temperature on the metabolic rate ($K(T)$) according to Eq. 16:

$$403$$

$$404 K(T) = K_o e^{\left(\frac{T_A - T_o}{T_o T}\right)} * \left[1 + e^{\left(\frac{T_{AL} - T_{AL}}{T - T_L}\right)} + e^{\left(\frac{T_{AH} - T_{AH}}{T - T_H}\right)} \right]^{-1} \quad (16)$$

405
 406 where, K_o is the reference reaction rate at 288 K, T_A is the Arrhenius temperature, T_o is the
 407 Reference temperature, T_{AL} and T_{AH} are the Arrhenius temperature at lower and upper
 408 boundary, respectively, T_L and T_H are the lower and upper boundary tolerance, respectively
 409 and T is the water temperature (simulated as a time series variable).

410
 411 The DEB model starts with the ingestion of PON ($mgN d^{-1}$) by the sea urchins. This is based
 412 on ingestion rate (\dot{j}_x) ($mgC d^{-1}$) divided by the C/N ratio of the aquaculture waste (Eq. 17).
 413 Ingestion rate is proportional to the surface area of the structural volume and follows type-II
 414 function response depending on the density of PON.

$$415$$

$$416 \dot{j}_x = K(T) * f * \{j_x\} * V^{2/3} \quad (17)$$

417
 418 where, $K(T)$ is a temperature dependent rate, $\{j_x\}$ is the maximum surface area-specific
 419 ingestion, V is the structural volume and f is the functional response that can range between 0
 420 and 1 and is given by:

421

422
$$f = \frac{X}{X+X_K} \quad (18)$$

423

424 The saturation coefficient (X_K), is analogous to a Michaelis-Menten constant, in this case
 425 being the food density at which the ingestion rate is half the maximum. For the calculation of
 426 the food density in the environment (X), the concentration of PON is converted to organic
 427 carbon concentration.

428

429 DEB models assume that the assimilation rate, (\dot{P}_A), is independent of the ingestion rate:

430

431
$$\dot{P}_A = K(T) * f * \{\dot{P}_{Am}\} * V^{2/3} \quad (19)$$

432

433 where, $K(T)$ is a temperature dependent rate, f is the functional response, $\{\dot{P}_{Am}\}$ is the
 434 maximum surface area specific assimilation and V is the structural volume.

435

436 The food that is ingested but not assimilated as biomass will be released to the environment as
 437 faeces or as excretion by diffusion. The DEB model enables estimation of the potential
 438 amounts of faeces released by the sea urchins by estimating the hourly production of faeces
 439 released into the surroundings using Eq. 20 for the faeces production in ($mgC d^{-1}$) and Eq.
 440 21 for the excretion rate in ($mgN d^{-1}$). Eq. 20 is then divided by the C/N ratio in order to
 441 calculate the amount of PON that is in the sea urchin faeces, which is assumed to be
 442 immediately added to the PON and DIN pools and is thus available for consumption by the
 443 sea urchins and seaweed, respectively.

444

445
$$\dot{F} = \dot{J}_x - \dot{P}_A / \mu_{cj} \quad (20)$$

446

447 where, \dot{J}_x is the consumption rate, \dot{P}_A is the assimilation rate and μ_{cj} is the ratio of carbon to
 448 energy content.

449

450
$$\dot{D}_{excr} = \left\{ \left[\dot{P}_c - (1 - k_R) * \frac{dE_R}{dt} - \mu_V * \rho * \frac{dV}{dt} \right] * Q + \dot{P}_A * (Q_S - Q)_+ \right\} / \mu_{cj} \quad (21)$$

451

452 where, \dot{P}_c is the catabolic rate, k_R are the reproductive reserves fixed in the eggs, E_R are the
 453 reproductive reserves, μ_V is the structural energy quota, ρ is the biovolume density, V is the
 454 structural volume, Q is the sea urchin N quota, \dot{P}_A is the assimilation rate, μ_{cj} is the ratio of
 455 carbon to energy content and Q_S is the sediment N quota (calculated as the ratio of organic
 456 nitrogen to organic carbon in the sediment). The *P. lividus* N quota (Q) was set to

457 127 mgN mgC⁻¹ (Tomas et al. 2005) and sediment N quota (Q_s) is site specific it was set to
 458 7, which is a representative value for an average Scottish salmon farm site.

459

460 The assimilated energy from the food enters the reserve pool. The energy density $[E]$ in an
 461 organism may vary between 0 and the maximum energy density $[E_m]$ depending on the food
 462 density in the environment.

$$463 \frac{d[E]}{dt} = \dot{P}_A - \dot{P}_c \quad (22)$$

464

465 where, \dot{P}_A is the assimilation and \dot{P}_c the catabolic rate.

466

467 The sea urchin catabolic rate (\dot{P}_c) denotes the energy utilised by the structural body and is
 468 given by:

469

$$470 \dot{P}_c = K(T) * \left[\frac{[E]}{[E_G] + K * [E]} \right] * \left(\frac{[E_G] * \{\dot{P}_{Am}\} * V^{2/3}}{[E_M]} + [\dot{P}_M] * V \right) \quad (23)$$

471

472 where, $K(T)$ is a temperature dependent rate, $[E]$ is the reserves, $[E_G]$ the volume specific
 473 cost of growth, K the catabolic flux to growth and maintenance, $\{\dot{P}_{Am}\}$ the maximum surface
 474 area specific assimilation, V the structural volume, $[E_M]$ the maximum reserve density and
 475 $[\dot{P}_M]$ the volume specific maintenance rate.

476

477 The rate of maintenance cost of the animals (\dot{P}_M) is proportional to the body volume and
 478 calculated with Eq. 24. Since the sea urchins will be mature the maturity maintenance P_j is
 479 also used Eq. 25:

480

$$481 \dot{P}_M = K(T) * [\dot{P}_M] * V \quad (24)$$

482

$$483 \dot{P}_j = \min(V, V_p) * [\dot{P}_M] * \frac{1-k}{k} \quad (25)$$

484

485 where, $K(T)$ is a temperature dependent rate, $[\dot{P}_M]$ is the volume specific maintenance rate, V
 486 is the structural volume, V_p is the structural volume at puberty and K is the catabolic flux to
 487 growth and maintenance.

488

489 The sea urchin structural volume growth (V) is given by:

490

491
$$\frac{dV}{dt} = \frac{(k \cdot \dot{P}_c - \dot{P}_M)_+}{[E_G]} \quad (26)$$

492

493 where, K is the catabolic flux to growth and maintenance, \dot{P}_c is catabolic rate, \dot{P}_M is the
 494 maintenance rate and $[E_G]$ is the volume specific cost of growth.

495

496 In this model we are also interested in the body mass (W) of the sea urchins, in order to
 497 calculate the total biomass of the stock. To convert volume to dry weight Eq. 27 is used:

498

499
$$W = V * \rho + \frac{(E + E_R * k_R)}{\mu_E} \quad (27)$$

500

501 where, V is the structural volume, ρ is the biovolume density, E and E_R are reserves and
 502 reproductive reserves, respectively, k_R are the reproductive reserves fixed in the eggs and μ_E is
 503 the reserve energy content.

504

505 The total biomass was calculated as individual weight multiplied by the number of
 506 individuals. Once an individual has reached the volume (V_p) at sexual maturity, a portion of
 507 the total energy reserve is stored in the sea urchin reproductive reserves (E_R):

508

509
$$\frac{dE_R}{dt} = (1 - k) * \dot{P}_c - \dot{P}_j \quad (28)$$

510

511 where, K is the catabolic flux to growth and maintenance, \dot{P}_c is the catabolic rate and \dot{P}_j is the
 512 maturity maintenance

513

514 The DEB model simulates the process within individuals. However for this model it is
 515 necessary to know how a non-reproducing stock (N) will decrease in size with time, due to
 516 mortality. The decrease of the sea urchin stock size is calculated in Eq. 29 where due to the
 517 planktonic nature of sea urchin larvae, it is assumed they will be dispersed from the IMTA
 518 site and thus reproduction will represent a net energy loss and restocking of the sea urchins
 519 will be necessary. However, the release of the larvae will contribute to restocking the native
 520 sea urchin population.

521

522
$$\frac{dN}{dt} = -\delta_r * N - \delta_h * N \quad (29)$$

523

524 where, δ_r and δ_h are the natural and harvest mortality of sea urchins, respectively. The harvest
525 mortality (δ_H) was zero and at the last time step of the simulation all sea urchins were
526 harvested, same as in the salmon and seaweed submodels. The natural mortality (δ_r) was set
527 to 0.00102 individuals d^{-1} for sea urchins with test diameter smaller than 2 cm and 0.00056
528 individuals d^{-1} for sea urchins with test diameter larger than 2 cm (Turon et al. 1995).

529

530 During the grow-out stage of *P. lividus* juveniles, the stocking density is approximately 400
531 individuals m^{-2} (Carboni, 2013). Space is not an issue for the organic extractive component of
532 the IMTA, since for the production of 560,525 individuals only 1,401 m^2 would be required
533 and this area would be directly underneath the fish cages and the seaweed rafts.

534

535

536 2.5 Assumptions and simplifications

537 The overall model's key assumption is that all nitrogen released by the various IMTA
538 components is dispersed homogeneously within a quantified water volume defined as the
539 IMTA site water volume (see section 2.3). It is also assumed that all the nitrogen available in
540 the IMTA site volume is in a form suitable for uptake; thus the model does not distinguish
541 between nitrate and ammonium. Correspondingly, the model does not take into account the
542 interactions between nitrate and ammonium within the environment and organisms, such as
543 the role of sediment and water in the nutrient dynamics or denitrification. The increase of
544 light limitation due to increased self-shading as the seaweed grows was not considered,
545 neither was the shading caused by phytoplankton. Data from Broch and Slagstad (2012) could
546 be used to derive a seaweed self-shading formula from which an add-on model could be used
547 to simulate the changes in k . In this study the light extinction coefficient (k) was a constant
548 ($k=1$). In the seaweed growth submodel the small biomass loss due to mechanical damage
549 caused by harvesting was not included. It is also assumed that nitrogen is the only nutrient
550 limiting seaweed growth. Additionally, the seaweed biomass used as initial biomass is

551 assumed to have an average $\left(\frac{N_{min} + N_{max}}{2}\right)$ N quota (this can be regulated by using
552 nitrogen deprived seedlings). When seaweed is harvested it is assumed that the N quota of the
553 harvested seaweed is equal to the maximum N quota due to the high availability of DIN in the
554 virtually closed system. The assumption that the seaweed harvested has this high nitrogen
555 quota might lead to overestimation of the bioremediation efficiency and the effect of lower N
556 quota at harvest was examined in the sensitivity analysis (Tables 5 and 10). From a farm
557 practice perspective it is assumed, that the relative position of the extractive organisms in
558 relation to the fish cages is such that it ensures high O_2 availability for the fish. For the

559 salmon growth model, excretion, faeces production and feed loss were assumed to be steady
560 during the 18 month production period while in reality they change as the fish grow.

561

562 2.6 Production specifications of the baseline simulation

563 The results presented are from the IMTA baseline simulation, which was parameterized using
564 data acquired from the literature and from commercial salmon farm sites. The environmental
565 data such as monthly variations in seawater temperature and irradiance were acquired from
566 empirical databases for the West coast of Scotland and the production-specific input data
567 from Scottish commercial salmon farm sites (Figs. 2 and 3). Typically, S1 smolts are
568 transferred to sea in spring (April-May), so April is set as simulation time 0 and the model
569 then runs for 18 months. The test scenario farm consists of nine 90 m circular salmon cages
570 with the extractive organisms placed in immediate proximity to those cages. The model
571 simulates a farm that produces 1,000 t of Atlantic salmon in 18 months on-growing, a farm
572 size representative of the Scottish industry (FAO, Scottish Fish Farm Production Survey
573 2011).

574

575 Insert Fig 2 and Fig 3

576

577 3 Results

578 3.1 Growth performance of IMTA components at the baseline simulation

579 The baseline simulation run estimated that the mean individual fish biomass after 540 days
580 (18 months) was 3.78 kg (Fig. 4a) and the salmon stock decreased by 16,525 individuals
581 from 280,883 to 264,358 individuals (Fig. 4b).

582

583 Insert fig. 4 here

584

585 During the 18-month production period, 348 t of seaweed and 50 t of sea urchins were
586 produced and harvested as well as the targeted 1000t of salmon (Table 2). The seaweed
587 achieved high growth rates, especially during the summer months (Fig. 5). The effect of the
588 growth limitation factors on the seaweed growth rate is presented in Fig. 6. The lower
589 seaweed growth rate during the first 300 days (10 months) of the simulation (Fig. 5) can be
590 mainly attributed to low levels of nitrogen available for uptake (Figs. 6 and 10). It is clear that
591 in the hypothetical baseline model scenario, during the first 300 days of the simulation
592 seaweed growth is mainly limited by the availability of nitrogen. Temperature limits growth
593 more during the colder months (October – April) while, the effect of light intensity is rather

594 stable throughout the year (Fig. 6). It should be emphasized here that site specific shading
595 caused by phytoplankton or seaweed self shading does not contribute to light limitation in the
596 baseline simulation (see section 2.5 for more details).

597

598 Insert Fig. 5 and fig. 6 here

599

600 The aim of the IMTA model developed was to achieve high bioremediation efficiency.
601 Sustaining the seaweed biomass at a high density at all times, using the harvesting instruction
602 (described at section 2.3), played an important role in achieving this (Fig. 7). The first
603 seaweed harvesting occurred 330 days after the simulation start, following which there was
604 enough nitrogen available due to the large size of the fish and the environmental conditions
605 were also favorable for the remaining seven months of the simulation (April – October) (Figs.
606 3 and 6) thus ensuring constant high growth rate and harvesting at 10-day intervals (Fig. 7).

607

608 Insert Fig.7 here

609

610 At the beginning of the IMTA simulation the site was stocked with 827,900 sea urchins.
611 During the 18-month production period 50 t (wet weight) of sea urchins of the species *P.*
612 *lividus* were produced with average test diameter 4.47 cm (Table 2, Fig. 8). As a result 1.01 t
613 of nitrogen were assimilated in the sea urchin biomass and removed from the ecosystem via
614 the process of harvesting.

615

616 Insert fig. 8 and fig. 9 here

617

618 3.2 Test scenario bioremediation potential

619 For the production of 1,000 t of salmon with average feed conversion ratio (FCR) of 1.02 and
620 feed nitrogen content 7.2%; the model shows that 80 t of nitrogen are introduced into the
621 system over the 540 day simulated production period. From this 80 t, only 38% will be
622 accumulated by the fish and incorporated into their biomass. The remaining 62%, which
623 under the production scenario described above (production of 1000t of salmon) is 49.6 t, will
624 be released into the environment as dissolved and particulate nitrogen. Under the
625 environmental conditions and production method of the test scenario the total nitrogen
626 released to the environment from the IMTA site would be 36% less (31.8 t instead of 49.6 t)
627 than what would have been released from a salmon monoculture farm of the same capacity. In
628 detail, the amount of nitrogen released from salmon monoculture would be 62% of the
629 exogenous nitrogen input but only 39% in the IMTA system since a large proportion of the

630 nitrogenous waste will be assimilated by the extractive organisms and removed from the
631 ecosystem via harvesting (Figs. 9 and 10). Fig. 10 shows the gradual increase in nitrogen
632 within the IMTA system over the simulated production period.

633

634 3.3 Sensitivity analysis

635 All biological, environmental and production parameters were analysed in terms of
636 uncertainty and their relative importance in the model. Due to the large number of input and
637 response variables used in the sensitivity analysis, the results for only those that were shown
638 to be the most sensitive parameters (absolute values) to operation of the model are
639 summarized in Tables 3 to 6. Those parameters were therefore classified as potential critical
640 assumptions and thus require accurate estimation and/or calibration.

641

642 In the salmon submodel, the growth and nutrient uptake is most sensitive to change in the
643 TGC and secondarily on variation in the FCR (Table 3).

644

645 Insert Table 3 here

646

647 In the seaweed submodel, all output variables were most sensitive to parameters affecting
648 growth and nutrient uptake either indirectly through nitrogen uptake and nitrogen content of
649 the seaweed tissues, wet/dry ratio and the culture depth or directly through maximum growth
650 rate, temperature and nitrogen input from salmon excretion. These results show the overall
651 importance of temperature and nitrogen uptake for seaweed growth (Table 4). All parameters,
652 apart from culture depth that was negatively correlated with seaweed biomass harvested, were
653 positively correlated with the output variables. Also, increasing parameter values mirrored the
654 effect on the model output of decreasing parameter values, which indicates that most
655 parameters affected growth linearly.

656

657 Insert Table 4 here

658

659 In the sea urchin submodel the output variables were most sensitive to parameters related to
660 temperature. Other sensitive parameters included the maximum surface-specific feeding rate
661 (Table 5), the volume specific cost of growth and the ratio of carbon to energy content. An
662 increase in the value of T_L had a strong negative effect on the output variable 'harvested sea
663 urchin biomass' (sensitivity -9.96), while a reduction caused a weak positive effect
664 (sensitivity 0.08). Overall, this analysis revealed that the DEB model was most sensitive to
665 increases in T_L . The model also showed a high sensitivity to increases or decreases in other

666 parameters (Table 5) while changes in the remaining DEB input variables had little effect on
667 growth (sensitivity < 1).

668

669 Insert Table 5 here

670

671 Table 6 summarizes tables 3 to 5 in the context of the overall model. The most sensitive
672 parameters within the salmon and seaweed sub-models are also the most sensitive to
673 outcomes of the overall model. The most sensitive parameters of the DEB sub-model do not
674 play such an important role within the overall model performance due to the sea urchin
675 biomass being very small in comparison to that of salmon and seaweed (Table 6).

676

677 Insert Table 6 here

678

679 4. Discussion

680 The aim of this study was the development of a dynamic tool for relative comparison of
681 different IMTA scenarios at a given production site, rather than the generation of absolute
682 bioremediation and production estimates. The model results presented are derived from a
683 baseline simulation, which can be re-parameterised to simulate different scenarios.

684

685 Results from IMTA studies similar to the one presented here, have shown bioremediation
686 potential of a similar scale to the output generated by the present model. Broch and Slagstad
687 (2012) estimated that 0.8 km² of *Saccharina latissima* biomass would be needed to sequester
688 all the waste released from a salmon farm producing 1,000 tonnes a year and Abreu et al.
689 (2009) estimated that a 1 km² *Gracilaria chilensis* farm would be needed to fully sequester
690 the dissolved nutrients released from a salmon farm producing 1,000 tonnes a year. Sanderson
691 et al. (2012) estimated that 0.01 km² of *S. latissima* could remove 5.3-10% of the dissolved
692 nitrogen released from a salmon farm producing 500 t of salmon in two years. However, the
693 results presented, as the results from any other IMTA model or trial, cannot be directly
694 compared with output from similar studies due to the fact that the productivity of an IMTA
695 farm depends on local environmental characteristics, the species combination used, the
696 duration of the grow out seasons and other factors. Moreover, linear interpolation of results
697 from studies with shorter durations can lead to misestimating results. Thus a large variance in
698 production and bioremediation results is natural. The results of this study are in the same
699 order of magnitude as the results acquired from the studies mentioned above; however they
700 suggest higher bioremediation potential, possibly largely due to the harvesting method
701 applied. Specifically, it was estimated that 35% of the total nitrogen released from a salmon

702 farm, with the specifications of the simulated scenario, will be accumulated by the 0.01 km²
703 of *Ulva* sp suggesting a very high bioremediation efficiency. Aiming to achieve 100%
704 bioremediation (i.e. no available nitrogen above the ambient concentration occurs at any
705 given time), especially without the addition of external feed sources for the extractive
706 organisms and while sustaining the quality of the extractive organisms, is unrealistic and
707 might only be possible in a fully closed system such as a Recirculating Aquaculture System
708 (RAS). Nonetheless, even at lower bioremediation efficiencies, the model already
709 demonstrates the environmental benefits of IMTA.

710

711 The simulated growth for juvenile and adult sea urchins showed good correspondence with
712 empirical data, although the reference temperature for which all the DEB constants were
713 calculated was 20°C (Table 2) which is significantly higher than the average temperature (11°
714 C) at the modelled IMTA site during the 18 month grow out period. The sea urchin growth
715 model output is comparable to the results of Cook and Kelly (2007) who concluded that *P.*
716 *lividus*, with an initial test diameter of 1 cm, deployed adjacent to fish cages need
717 approximately 3 years to reach market size (> 5.5 cm test diameter). The sea urchins will be
718 around 1 year old when they are deployed and 2.5 years old at the end of the grow out phase
719 at which point their test diameter will be 4.47 cm. At the end of the 18-month grow-out phase
720 of the salmon, the sea urchins will have reached the lower limit of their target market size.
721 The growth rate achieved in this study was similar to that achieved directly adjacent to the sea
722 cages (Cook and Kelly, 2007) and higher than that achieved by Fernandez and Clatagirone
723 (1994) (1.41 mm per month) where the sea urchins were fed with artificial feed containing
724 fish meal and fish oil at higher water temperature than this study (5-33°C). After the sea
725 urchins have reached market size a two to three month period of market conditioning at
726 controlled environment is required (Carboni, 2013; Grosjean et al. 1998).

727

728 In the first eight to ten months of the IMTA baseline scenario, seaweed and sea urchin growth
729 is limited by nitrogen (Figs. 6 and 8b), since the fish are still small and thus require a
730 relatively low feed input. From the eleventh month onwards mainly light and to a lower
731 extend temperature are limiting the seaweed growth. From that point onwards the seaweed
732 growth rate is high as can be seen in Fig. 5. For successful high bioremediation efficiency, at
733 an IMTA farm seaweed growth should not be limited by light or temperature but only by
734 nutrient availability. For this reason IMTA systems could be more efficient in sites further
735 south than the one used for the baseline simulation. It can be seen clearly in Fig. 10 that there
736 is a constant increase of the residual DIN and PON remaining at the IMTA site. This high
737 waste output particularly during the last months of the salmon production is a challenge for

738 achieving very high bioremediation efficiency. The ratio of salmon to extractive organisms
739 (especially for sea urchins) used at the test scenario is very low (Table 2). From the
740 perspective of space requirement there is the potential for increase of the amount of sea
741 urchins produced, however the quantity of waste available for consumption by the sea urchins
742 decreases with distance from the sea cages and thus increasing the production would mean
743 that some sea urchins would be potentially too far from the food source. Furthermore, limited
744 market demand for marine invertebrates might also pose limitations.

745

746 The results of the sensitivity analysis indicate that the model is robust, since variation of key
747 model parameters by $\pm 10\%$ does not cause unexpected changes in the effect parameters. The
748 various model parameters have a different relative influence on the model's output, both in
749 terms of harvestable biomass and in terms of nitrogen bioremediation. Thus, depending on
750 users' specific study objectives, one should consider the precision with which certain
751 parameter values are determined, and whether further tuning is required. This model
752 sensitivity analysis is a useful means for assessing which are the key parameters that increase
753 model uncertainty. Those parameters with high sensitivity have a big impact on the output of
754 the model (e.g. thermal sensitivity parameters T_L in the sea urchin DEB submodel, T in all the
755 submodels and μ_{max} in the seaweed submodel), and therefore future efforts should focus on
756 methods for improving their estimation. In contrast, because parameters with low sensitivity
757 have little influence on the output of the model, their estimation could be simplified.
758 Consequently, despite the large variability observed in some of the parameters, their relative
759 importance may be minor if their sensitivity is low.

760

761 The model presented here is highly adaptable as all the submodels can function
762 independently. By altering model variables the submodels can simulate growth and nutrient
763 assimilation under different environmental conditions or for different species. Altering the
764 values of constants can also help assess their effect on the IMTA system and in some cases
765 these values can be optimised. For example, all the values related with production practices at
766 the IMTA site, such as seaweed harvesting frequency, maximum seaweed biomass allowed,
767 initial biomass of seaweed or sea urchins, seaweed culture depth and seaweed density, can be
768 optimised for the achievement of higher bioremediation efficiency and/or higher extractive
769 organism production.

770

771 Apart from achieving the major objectives described the model can be used for the
772 accomplishment of more general objectives such as: optimization of IMTA culture practices
773 (e.g. timing and sizes for seeding and harvesting, in terms of total production), assessment of

774 the role of IMTA in nutrient waste control and used as input for the evaluation of economic
775 efficiency of various system designs. The present model can be used as a decision support
776 tool for open-water IMTA only after being coupled with waste distribution modelling and
777 environmental sampling for model parameterization. Future versions of the model can link the
778 virtually closed IMTA system to hydrodynamic models for spatial analysis of the waste
779 dispersion and nutrient dilution. Such a model could help develop a balance among the
780 components of the IMTA system and assist in developing an IMTA design for maximum
781 waste uptake in “open environment systems”, as water exchange rate is the key factor
782 influencing the assimilative performance, thus enabling prediction of the effectiveness and
783 productivity of open water IMTA systems.

784

785 Acknowledgements

786

787 This PhD study was funded by the Marine Alliance of Science and Technology, by the
788 Institute of Aquaculture, University of Stirling and by IKY State Scholarships Foundation of
789 Greece.

790

791

792 References

793

- 794 Abreu, H., Varela, D.A., HenriÁLquez, L., Villaroel, A., Yarish, C., Sousa-Pinto, I.,
795 Buschmann, A.H., 2009. Traditional vs. integrated multi-trophic aquaculture of
796 *Gracilaria chilensis* C. J. Bird, J. McLachlan & E. C. Oliveira: productivity and
797 physiological performance. *Aquaculture*. 293 (3-4), 211–220.
- 798 Angell, A.R., Pirozzi, I., de Nys, R., Paul, N.A., 2012. Feeding preferences and the nutritional
799 value of tropical algae for the abalone *Haliotis asinine*. *PLoS ONE*, 7 (6), art. No.
800 e38857.
- 801 Austreng, E., Storebakken, T., Åsgård, T., 1987. Growth rate estimates for cultured Atlantic
802 salmon and rainbow trout. *Aquaculture*. 60, 157–160.
- 803 Aveytua-Alcázara, L., Camacho-Ibara, V.F., Souzab, A.J., Allenc, J.I., Torres, R., 2008.
804 Modelling *Zostera marina* and *Ulva sp.* in a coastal lagoon. *Ecol. Model.* 218, 354–
805 366.
- 806 Bjornsater, B.R., Wheeler, P.A., 1990. Effect of nitrogen and phosphorus supply on growth
807 and tissue composition of *Ulva fenestrata* and *Enteromorpha intestinalis* (*Ulvales*
808 *Chlorophyta*). *J. Phycol.* 26, 603-611.

809 Brett, J.R., 1979. Environmental Factors and Growth, in: Hoar, W.S., Randall, D.J., Brett,
810 J.R. (Eds.), Fish Physiology VIII. Academic Press, New York, pp. 599–675.

811 Broch, O., Slagstad, D., 2012. Modelling seasonal growth and composition of the kelp
812 *Saccharina latissima*. J. Appl. Phyc. 24, 759–776.

813 Broch, O.J., Ellingsen, I.H., Forbord, S., Wang, X., Volent, Z., Alver, M.O., Handå, A.,
814 Andresen, K., Slagstad, D., Reitan, K.I., Olsen, Y., Skjermo, J., 2013. Modelling the
815 cultivation and bioremediation potential of the kelp *Saccharina latissima* in close
816 proximity to an exposed salmon farm in Norway. Aquaculture Environmental
817 Interactions 4, 186–206.

818 Carboni, S., 2013. Research and development of hatchery techniques to optimize juvenile
819 production of the edible Sea Urchin, *Paracentrotus lividus*. PhD. Thesis. University of
820 Stirling, UK.

821 Chopin, T., Buschmann, A. H., Halling, C., Troell, M., Kautsky, N., Neori, A., Kraemer, G.
822 P., Zertuche-González, J. A., Yarish, C. and Neefus, C., 2001. Integrating seaweeds
823 into marine aquaculture systems: a key toward sustainability. J. Phycol. 37, 975–986.

824 Coffaro, G., Sfriso, A., 1997. Simulation model of *Ulva rigida* growth in shallow water of the
825 Lagoon of Venice. Ecol. Model. 102, 55-66.

826 Cohen, I., Neori, A., 1991. *Ulva lactuca* biofilters for marine fishpond effluents. Bot. Mar. 34,
827 475-482.

828 Cook, E.J., Kelly, M.S., 2007. Enhanced production of the sea urchin *Paracentrotus lividus* in
829 integrated open-water cultivation with Atlantic salmon *Salmo salar*. Aquaculture. 273
830 (4), 573-585.

831 Corner, R., Brooker, A., Telfer, T., Ross, L.G., 2006. A fully integrated GIS-based model of
832 particulate waste distribution from marine fish-cage sites. Aquaculture. 258, 299–311.

833 Droop, M., 1968. Vitamin B12 and marine ecology. IV. The kinetics of uptake, growth and
834 inhibition in *Monochrysis Lutheri*. J. Mar. Biol. 48, 689–733.

835 Dumas, A., France, J., Bureau, D., 2010. Modelling growth and body composition in fish
836 nutrition: where have we been and where are we going?. Aquaculture Research. 41-2,
837 161–181.

838 FAO, 2011. Scottish Fish Farm Production Survey 2011.
839 <http://www.scotland.gov.uk/Resource/0040/00401446.pdf> [21 May 2014]

840 Fei, X.G., Lu, S., Bao, Y., Wilkes, R., Yarish, C., 1998. Seaweed cultivation in China. World
841 Aquaculture 29, 22–24.

842 Fernandez, C.M., Caltagirone, A., 1994. Growth rate of adult *Paracentrotus lividus* in a
843 lagoon environment: the effect of different diet types, in: David, B., Guille, A., Feral,

844 J.P., Roux, M. (Eds.), Echinoderms Through Time. Balkema, Rotterdam, pp. 655–
845 660.

846 Fujita, R.M., 1985. The role of nitrogen status in regulating transient ammonium uptake and
847 nitrogen storage by macroalgae. *J. Exp. Mar. Biol. Ecol.* 92, 283-301.

848 Gillibrand, P.A., Gubbins, M.J., Greathead, C., Davies, I.M., 2002. Scottish Executive
849 locational guidelines for fish farming: predicted levels of nutrient enhancement and
850 benthic impact. Scottish Fisheries Research Report Number 63 / 2002 Fisheries
851 Research Services, Marine Laboratory, Aberdeen.

852 Grosjean, P., 2001. Growth model of the reared sea urchin *Paracentrotus lividus* (Lamarck,
853 1816). PhD thesis. Universite Libre de Bruxelles, Belgium.

854 Iwama, G.K., and Tautz A.F., 1981. A Simple Growth Model for Salmonids in Hatcheries.
855 *Can. J. Fish. Aquat. Sci.* 38(6), 649-656.

856 Jiang, Z.J., Fang, J.G., Mao, Y.Z., Wang, W., 2010. Eutrophication assessment and
857 bioremediation strategy in a marine fish cage culture area in Nansha Bay. *J. Appl.*
858 *Phyc.* 22, 421–426.

859 Jobling, M., 2003. The thermal growth coefficient (TGC) model of fish growth: a cautionary
860 note. *Aquaculture Research.* 34, 581-584.

861 Kelly, M.S., Brodie, C.C., McKenzie, J.D., 1998. Somatic and gonadal growth of the sea
862 urchin *Psammechinus miliaris* (Gmelin) maintained in polyculture with the Atlantic
863 salmon. *J. Shellfish Res.* 17, 1557–1562.

864 Kooijman, S.A.L.M., 1986. Energy budgets can explain body size relations. *J. Theor. Biol.*
865 121, 269–282.

866 Kooijman, S.A.L.M., 2000. *Dynamic Energy and Mass Budgets in Biological Systems.* CUP,
867 Cambridge.

868 Kooijman, S.A.L.M., 2001. Quantitative aspects of metabolic organization: a discussion of
869 concepts. *Phil. Trans. Royal Soc. London B: Biol. Sci.* 356, 331–349.

870 Kooijman, S.A.L.M., 2008. *Dynamic Energy Budget theory for metabolic organization.* Third
871 Edition CUP, Cambridge.

872 Kooijman, S.A.L.M., 2014. Add_my_pet: *Paracentrotus lividus*. URL:
873 http://www.bio.vu.nl/thb/deb/deblab/add_my_pet/html/Paracentrotus_lividus.html
874 [21 May 2014]

875 Lapointe, B.E., Tenore, K.R., 1981. Experimental outdoor studies with *Ulva fasciata Delile I.*
876 Interaction of light and nitrogen on nutrient uptake, growth and biochemical
877 composition. *J. Exp. Mar. Biol. Ecol.* 92, 135-152.

878 Lobban, C.S., Harrison P.J., 1994. *Seaweed Ecology and Physiology.* CUP, Cambridge.

879 Luo, M.B., Liu, F., Xu, Z.L., 2012. Growth and nutrient uptake capacity of two co-occurring
880 species, *Ulva prolifera* and *Ulva linza*. *Aquat. Bot.* 100, 18-24.

881 Marine Harvest, 2012. Salmon farming industry handbook.
882 <http://www.marineharvest.com/PageFiles/1296/2012%20Salmon%20Handbook%201>
883 [8.juli_h%C3%B8y%20tl.pdf](http://www.marineharvest.com/PageFiles/1296/2012%20Salmon%20Handbook%201) [30 April 2014]

884 Marine Scotland, 2013. Draft Seaweed Policy Statement Consultation Paper.
885 <http://www.scotland.gov.uk/Publications/2013/08/6786> [1 June 2014]

886 Neori, A., Chopin, T., Troell, M., Buschmann, A.H., Kraemer, G.P., Halling, C., Shipgel, M.,
887 Yarish C., 2004. Integrated aquaculture: rationale, evolution and state of the art
888 emphasizing seaweed biofiltration in modern mariculture. *Aquaculture*. 231, 361–
889 391.

890 Neori, A., Cohen, I., Gordin, H., 1991. *Ulva lactuca* biofilters for marine fishpond effluents.
891 II. Growth rate, yield and C:N ratio. *Bot. Marina*. 34, 483-489.

892 Perrot, T., Rossi, N., Ménesguen, A., Dumas, F., 2014. Modelling green macroalgal blooms
893 on the coasts of Brittany, France to enhance water quality management. *J. Mar.*
894 *Syst.* 132, 38-53.

895 Raven, J.A., Geider, R.J., 1988. Temperature and algal growth. *New Phytol.* 110, 441-461.

896 Reid, G.K., Chopin, T., Robinson, S.M.C., Azevedo, P., Quinton, M., Belyea, E., 2013.
897 Weight ratios of the kelps, *Alaria esculenta* and *Saccharina latissima*, required to
898 sequester dissolved inorganic nutrients and supply oxygen for Atlantic salmon, *Salmo*
899 *salar*, in Integrated Multi-Trophic Aquaculture systems. *Aquaculture*. 408/409, 34-46.

900 Sanderson, J.C., Dring, M.J., Davidson, K., Kelly, M.S., 2012. Culture, yield and
901 bioremediation potential of *Palmaria palmata* (Linnaeus) Weber & Mohr and
902 *Saccharina latissima* (Linnaeus) C. E. Lane, C. Mayes, Druehl & G. W. Saunders
903 adjacent to fish farm cages in northwest Scotland. *Aquaculture*. 354/355, 128–135.

904 Solidoro, C., Pecenic G., Pastres, R., Franco D., Dejak, C., 1997. Modelling macroalgae
905 (*Ulva rigida*) in the Venice lagoon: Model structure identification and first
906 parameters estimation, *Ecol. Model.* 94 (2–3), 191-206.

907 Soto, D., Aguilar-Manjarrez, J., Hishamunda, N., 2008. Building an ecosystem approach to
908 aquaculture. FAO/Universitat de les Illes Balears Expert Workshop. 7–11 May 2007,
909 Palma de Mallorca, Spain. FAO Fisheries and Aquaculture Proceedings. No. 14.
910 Rome, FAO.

911 Steele, J.H., 1962. Environmental control of photosynthesis in the sea. *Limnol. Oceanogr.*, 7,
912 137–150

913 Tomas, F., Romero, X., Turon, X., 2005. Experimental evidence that intra-specific
914 competition in seagrass meadows reduces reproductive potential in the sea urchin
915 *Paracentrotus lividus* (Lamarck). *Sci Mar.* 69, 475–484.

916 Trancoso, A.R., Saraira, S., Fernandes, L., Pina, P., Leitao, P., Neves, R., 2005. Modelling
917 macroalgae using a 3D hydrodynamic-ecological model in a shallow, temperate
918 estuary. *Ecol. Model.* 187, 232-246.

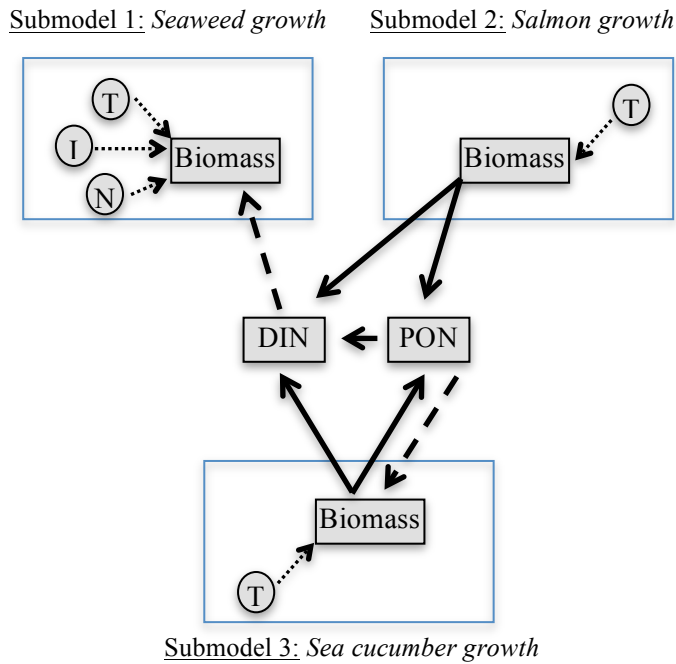
919 Turon, X., Giribet, G., López, S., Palacín, C., 1995. Growth and population structure of
920 *Paracentrotus lividus* (Echinodermata: Echinoidea) in two contrasting habitats. *Mar.*
921 *Ecol. Prog. Ser.* 122, 193-204.

922 Wang, X., Broch, O.J., Forbord, S., Handå, A., Skjermo, J., Reitan, K.I., Vadstein, O., Olsen,
923 Y., 2013. Assimilation of inorganic nutrients from salmon (*Salmo salar*) farming by
924 the macroalgae (*Saccharina latissima*) in an exposed coastal environment:
925 implications for integrated multi-trophic aquaculture. *J. Appl. Phyc.* DOI
926 10.1007/s10811-013-0230-1

927 Wang, X., Olsen, L.M., Reitan, K.I., Olsen, Y., 2012. Discharge of nutrient wastes from
928 salmon farms: environmental effects, and potential for integrated multi-trophic
929 aquaculture. *Aquaculture Environmental Interactions.* 2, 267-283.

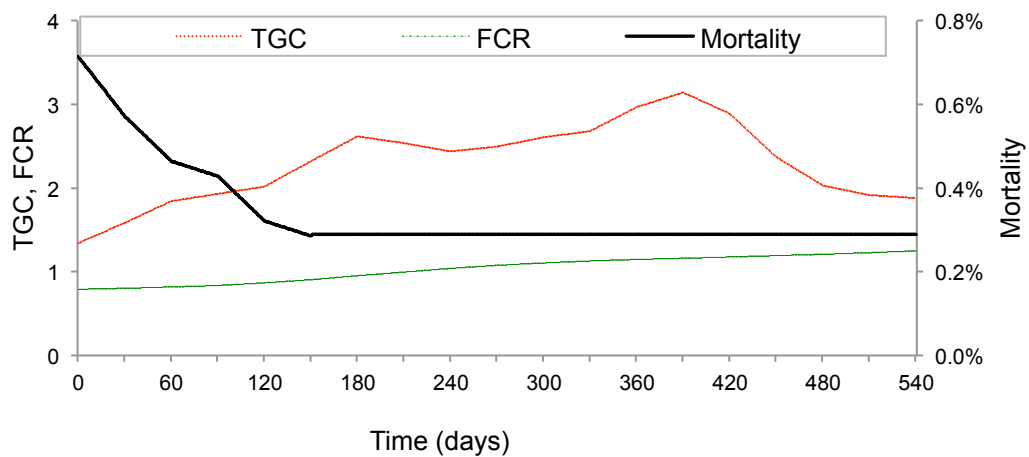
930 Zaldívar, J.M., Bacelar, F.S., Dueria, S., Marinova, D., Viaroli, P., Hernández-García E.,
931 2009. Modeling approach to regime shifts of primary production in shallow coastal
932 ecosystems. *Ecol. Model.* 220, 3100-3110.

933



934
935
936
937
938
939
940
941

Fig. 1: Conceptual diagram of the model showing the major state variables (squares) and forcing functions (circles) of each submodel as well as the interactions among the submodels. The dashed lines represent nitrogen assimilation and the solid lines nitrogen release. *T*, *I* and *N* represent temperature, irradiance and nitrogen, respectively.



942
943
944
945
946
947
948

Fig. 2: Production scenario values of the time series variables, TGC, FCR and salmon mortality.

949
950
951
952
953
954
955
956
957
958
959
960
961
962

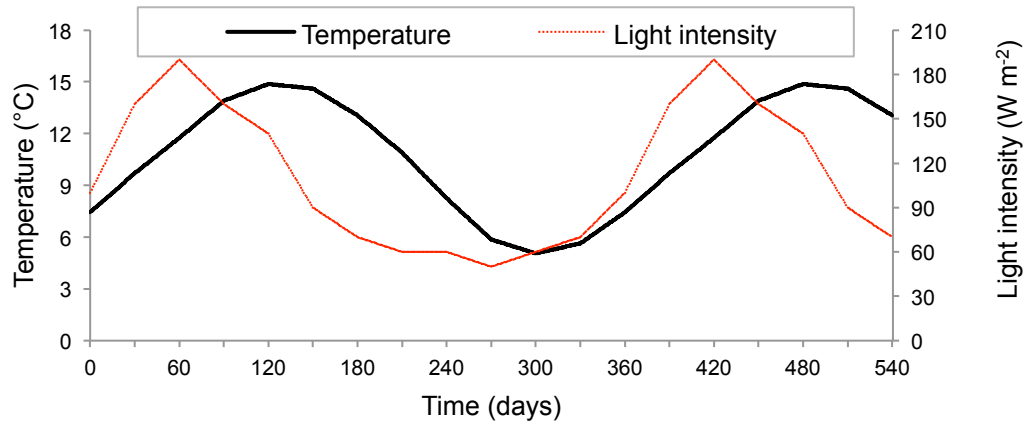
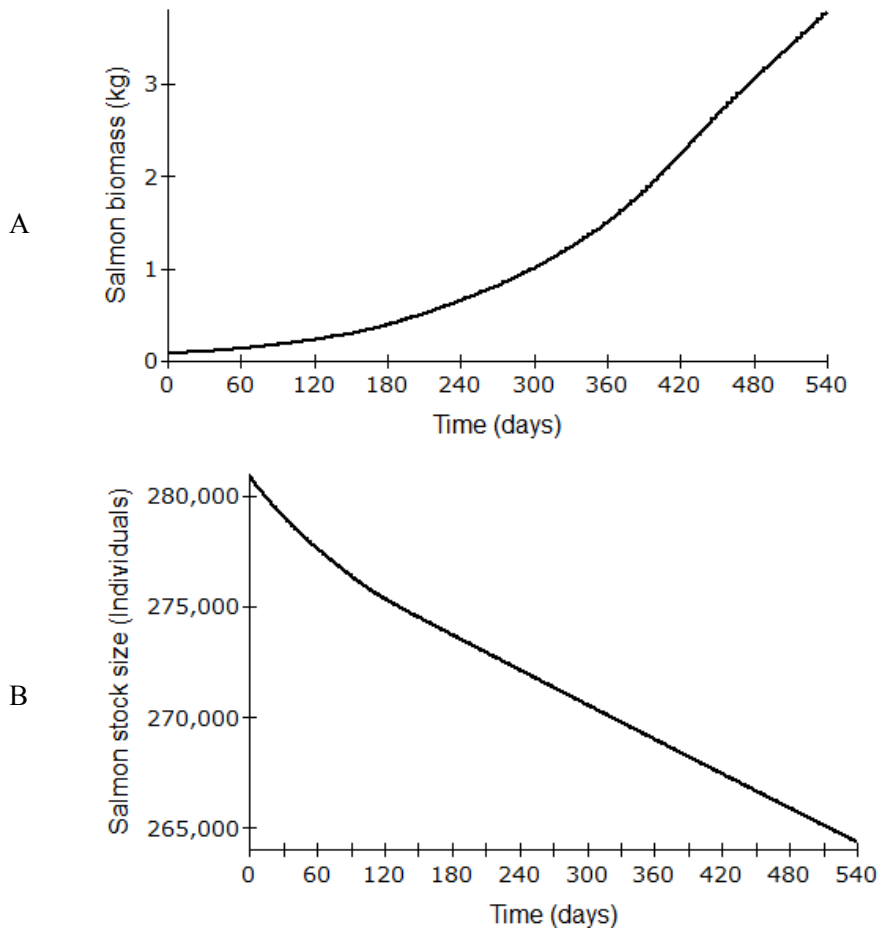
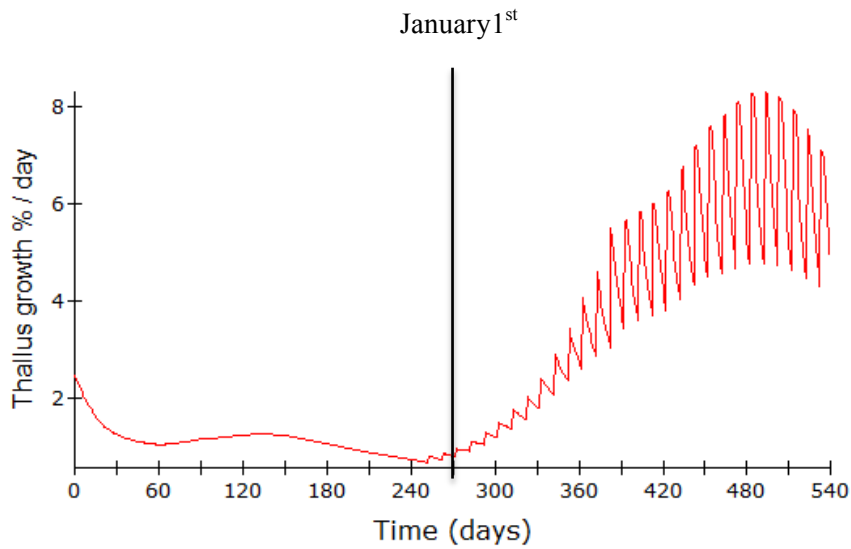


Fig. 3: Production scenario values of the time series variables, water temperature and light intensity.

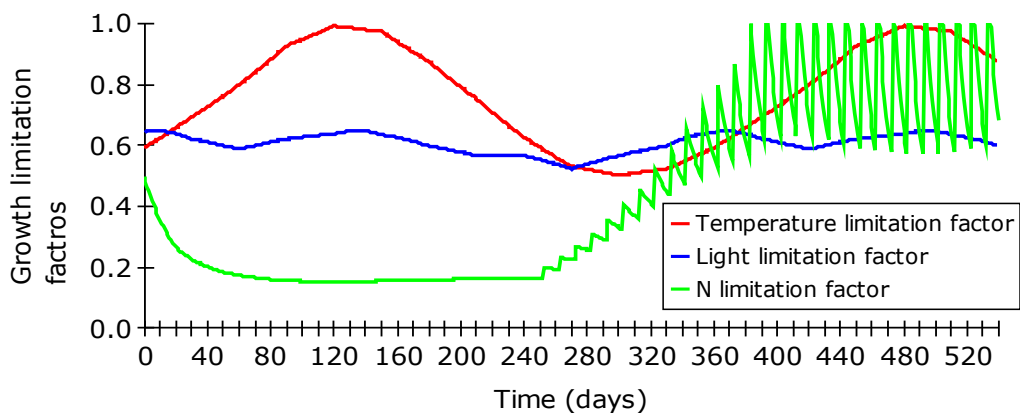


963 Fig. 4: Simulated output of the salmon: a) individual average biomass, b) stock size, during
964 the 540 days of culture at sea.
965



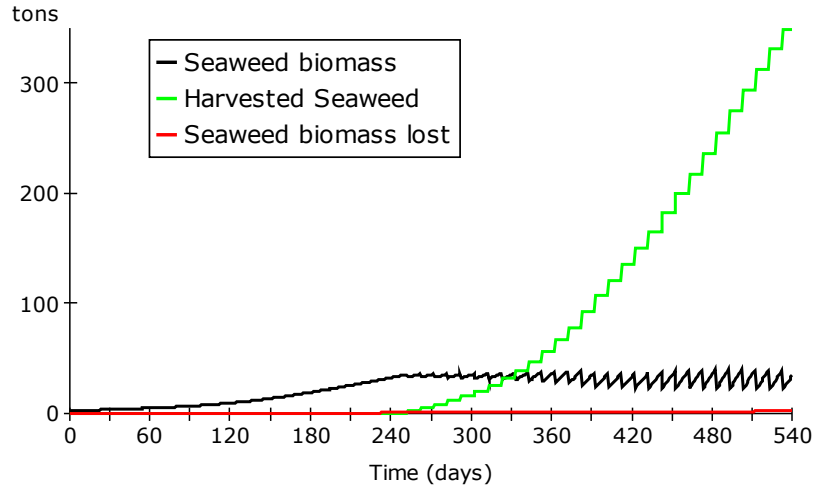
966
 967
 968
 969
 970
 971
 972

Fig. 5: Seaweed specific growth rate for *Ulva* sp. during the test scenario production conditions.



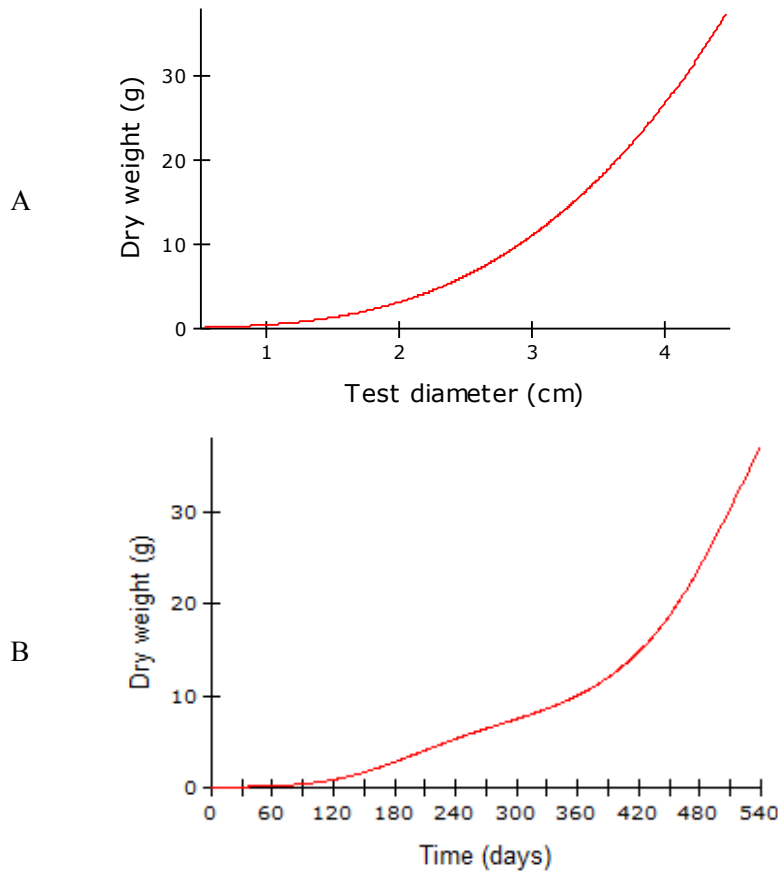
973
 974
 975
 976
 977
 978

Fig. 6: Seaweed growth limitation factors, under the test scenario production conditions. The limitation factors can vary between 0 and 1; where a value of 1 means that the factor does not inhibit growth.



979
 980
 981
 982
 983
 984

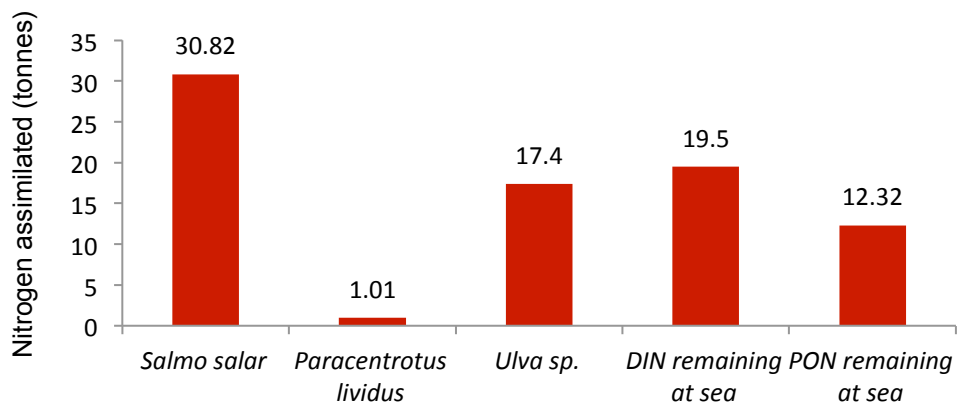
Fig. 7: Seaweed submodel simulation output for *Ulva* sp. produced under the test scenario conditions. It illustrates the biomass change over time, the cumulative amount of seaweed biomass lost due to natural causes and the cumulative amount of seaweed biomass harvested.



985
 986
 987

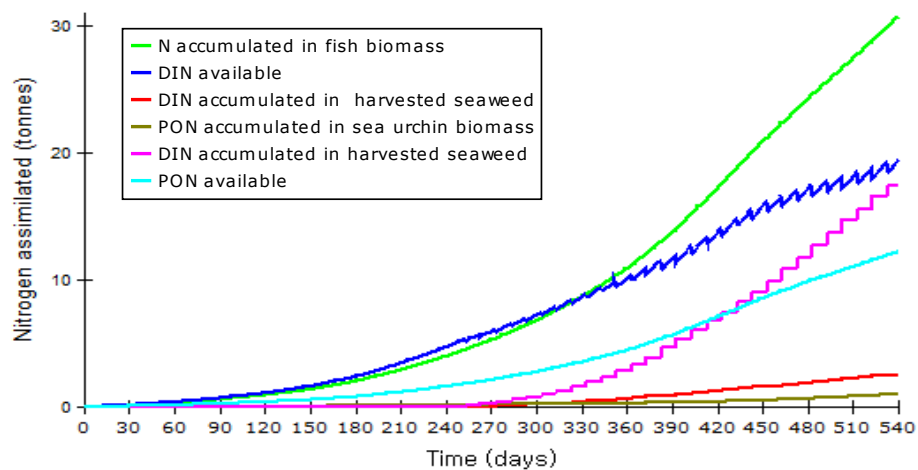
Fig. 8: Sea urchin submodel simulation output for: a) the length - dry weight relationship of *P. lividus* b) *P. lividus* dry weight

988



989

990 Fig. 9: Modelled output of nitrogen assimilated (in harvested biomass) in the different IMTA
991 components and the amount of DIN or PON remaining at the virtually closed IMTA site area
992 (above the ambient seawater nutrient concentration) over a 540 day simulated production
993 period.



994

995

996 Fig. 10: Modelled output of cumulative amount of nitrogen assimilated by the different IMTA
997 components and the amount of DIN or PON remaining at the IMTA site area at each time
998 step.

999

Table 1: Parameterization of constants and time series variables used at the seaweed growth submodel.

Variable	Description	Value		Units	Reference
		range in literature	Value used		
μ_{max}	Maximum growth rate	0.8-18	10	% Day ⁻¹	Neori et al., 1991; Luo et al., 2012; Perrot et al., 2014
N_{max}	Maximum intracellular quota for N	36-54	50	mg ⁻¹ N g dw ⁻¹	Fujita, 1985; Bjornsater and Wheeler, 1990; Cohen and Neori 1991; Perrot et al., 2014
N_{min}	Minimum intracellular quota for N	10 to 13	10	mg ⁻¹ N g dw ⁻¹	Fujita, 1985; Bjornsater and Wheeler, 1990; Cohen and Neori 1991; Perrot et al., 2014
T	Water Temperature	Site specific	6.8-13.7*	°C	n/a
q_{10}	Seaweed temperature coefficient	2	2	n/a	Aveytua-Alcázara et al., 2008
I_0	Water surface light intensity	Site specific	50-190*	W m ⁻²	n/a
I_{opt}	Optimum light intensity for macroalgae	50	50	W m ⁻²	Perrot et al., 2014
k	Light extinction coefficient	Site specific	1	m ⁻¹	n/a
z	Culture depth	Farm practice	2	m	n/a
V_{max}	Maximum N uptake rate	0.44-2.2	1.32	mgN g ⁻¹ dw h ⁻¹	Lapointe and Tenore 1981; Perrot et al., 2014
K_N	N half saturation	0.06-0.55	0.31	mg L ⁻¹	Perrot et al., 2014
Wet/Dry	Wet to dry weight ratio	6.7-10.15	8.43	n/a	Neori et al., 1991; Angell et al., 2012
M	Mortality	0.009-0.02	0.015	d ⁻¹	Aveytua-Alcázara et al., 2008; Perrot et al., 2014
T_{ref}	Reference temperature for seaweed growth	n/a	15	°C	Neori et al., 1991; Luo et al., 2012; Perrot et al., 2014

	Decomposition				
Ω	rate and natural biomass loss	n/a	M / 2	d ⁻¹	n/a
	Loss rate due to environmental disturbance				
D	DIN concentration in sea water	n/a	M / 2	d ⁻¹	n/a
	Site specific				
S	0.594 mg m ⁻³				n/a

1001 * Time series variable

1002

1003

1004 Table 2: Test scenario output illustrating the initial and final wet biomass of each IMTA
 1005 component, as well as the salmon to extractive organism weight ratios required for achieving
 1006 the bioremediation effect described above.

1007

Biomass (wet)	Initial (tonnes)	Final (tonnes)
<i>Ulva sp.</i>	2	348
<i>P. lividus</i>	0.09	50
<i>Salmo salar</i>	22.47	1000
Ratio		
<i>Salmo salar</i> / <i>Ulva sp.</i>	11.24	2.87
<i>Salmo salar</i> / <i>P. lividus</i>	249.67	20

1008

1009

1010

1011 Table 3: Most sensitive parameters (with $NS \geq 1$) for the effect variables *N accumulated in*
1012 *harvested salmon* and *Harvested salmon biomass*, by descending absolute normalized
1013 sensitivity coefficient (NS) for either + or – 10% of the effect parameter’s value. The baseline
1014 values of the effect variables *N accumulated in harvested salmon* and *Harvested salmon*
1015 *biomass* were 30.82 and 1000 tonnes, respectively.

1016

Parameter symbol	Parameter name	Parameter baseline value	Effect for parameter + 10%	NS for parameter +10%	Effect for parameter -10%	NS for parameter -10%
<i>N accumulated in harvested salmon: effect baseline value is 30.82 tonnes</i>						
TGC	Thermal-unit growth coefficient*	2.33	38.24	2.41	24.42	2.08
FCR	Feed conversion ratio*	1.04	33.91	1	27.74	1
<i>Harvested salmon biomass: effect baseline value is 1000 tonnes.</i>						
TGC	Thermal-unit growth coefficient*	2.33	1233	2.33	798	2.02

1017

1018

1019 Table 4: Most sensitive parameters (with $NS \geq 1$) for the effect variables *DIN accumulated in*
 1020 *harvested seaweed* and *harvested seaweed biomass*, by descending absolute NS value for
 1021 either + or – 10% of the effect parameter’s value. The baseline values of the effect variables
 1022 *DIN accumulated in harvested seaweed* and *Harvested seaweed biomass* were 17.55 and
 1023 347.97 tonnes, respectively.

Parameter symbol	Parameter name	Parameter baseline value	Effect for parameter + 10%	NS for parameter +10%	Effect for parameter - 10%	NS for parameter -10%
<i>DIN accumulated in harvested seaweed: effect baseline value is 17.55 tonnes</i>						
N_{state}	Nutrient state of seaweed at harvest**	10	3.63	-7.93	10.59	3.97
μ_{max}	Max seaweed growth rate	0.13	21.38	2.18	13.96	2.05
T	Water Temperature*	10.89	21	1.97	14.83	1.55
V_{max}	Maximum N uptake rate	1.32	19.98	1.38	14.59	1.69
W/D	Wet / dry ratio	8.43	20	1.40	14.68	1.64
z	Culture depth	2	20	1.40	15.41	1.22
N_{excr}	Nitrogen lost via excretion	0.45	18.25	0.40	15.64	1.09
<i>Harvested seaweed biomass: effect baseline value is 347.97 tonnes</i>						
μ_{max}	Max seaweed growth rate	0.13	424.57	2.20	293.53	1.56
T	Water Temperature*	10.89	416.95	1.98	293.60	1.56
V_{max}	Maximum N uptake rate	1.32	396.47	1.39	288.71	1.70
W/D	Wet / dry ratio	8.43	397.21	1.42	290.29	1.66
z	Culture depth	2	296.91	-1.47	305.13	1.23
N_{min}	Min intracellular quota for N	10	320.95	-0.78	387.64	-1.14
N_{max}	Max intracellular quota for N	50	327.78	-0.58	387.43	-1.13

1024

1025 Table 5: Most sensitive parameters (with $NS \geq 1$) for the effect variables *Nitrogen*
 1026 *accumulated in harvested sea urchin biomass* and *Harvested sea urchin biomass*, by
 1027 descending absolute NS value for either + or - 10% of the effect parameter's value. The
 1028 baseline values of the effect variables *Nitrogen accumulated in harvested sea urchin biomass*
 1029 and *Harvested sea urchin biomass* were 1.01 and 20.86 tonnes, respectively.
 1030

Parameter symbol	Parameter name	Parameter baseline value	Effect for parameter +10%	NS for parameter +10%	Effect for parameter -10%	NS for parameter -10%
<i>Nitrogen accumulated in harvested sea urchin biomass: effect baseline value is 1.01 tonnes</i>						
T	Water Temperature*	10.89	11.98	3.46	9.8	2.58
{Px}	Maximum surface-specific feeding rate	578.55	1.21	2.9	0.71	2.44
K_o	Reference reaction rate at 288 K	1	1.19	2.72	0.72	2.33
T_A	<i>P. lividus</i> Arrhenius temperature	8000	0.77	-1.74	1.14	-2.13
$[E_G]$	Volume specific cost of <i>P. lividus</i> growth	2748	0.82	-1.23	0.94	-0.01
μ_{cj}	Ratio of carbon to energy content	83.30	0.85	-0.91	1.04	-1.10
<i>Harvested sea urchin biomass: effect baseline value is 20.86 tonnes</i>						
T_L	<i>P. lividus</i> lower boundary tolerance	273	0.09	-9.96	21.02	-0.08
T	Water Temperature*	10.89	27.77	3.31	15.65	2.50
{Px}	Maximum surface-specific feeding rate	578.55	26.95	2.92	15.76	2.44
K_o	Reference reaction rate at 288 K	1	26.30	2.61	16.16	2.25
T_A	<i>P. lividus</i> Arrhenius temperature	8000	17.36	-1.68	25.14	-2.05
$[E_G]$	Volume specific cost of <i>P. lividus</i> growth	2748	17.96	-1.39	21.48	-0.30

1031
 1032

1033 Table 6: Most sensitive parameters (with $NS \geq 1$) for the effect variables *DIN available at the*
 1034 *IMTA site* and *PON available at the IMTA site*, by descending absolute NS value for either +
 1035 or - 10% of the effect parameter's value. The baseline value of the effect variables *DIN*
 1036 *available at the IMTA site* and *PON available at the IMTA site* were 19.50 and 12.32 tonnes,
 1037 respectively.
 1038

Parameter symbol	Parameter name	Parameter baseline value	effect for parameter + 10%	NS for parameter +10%	effect for parameter - 10%	NS for parameter -10%
<i>DIN available at the IMTA site: effect baseline value is 19.50 tonnes.</i>						
N_{state}	Nutrient state of seaweed at harvest**	10	33.41	7.13	26.45	-3.56
TGC	Thermal-unit growth coefficient*	2.33	27.72	4.22	12.34	3.67
FCR	Feed conversion ratio*	1.04	22.51	1.54	15.59	2.01
N_{excr}	Nitrogen lost via excretion	0.45	22.45	1.51	15.64	1.98
μ_{max}	Max seaweed growth rate	0.13	15.67	-1.96	23.08	-1.84
$N_{content}$	Nitrogen content in feed	0.07	22.41	1.49	15.68	1.96
T	Water Temperature*	10.89	16.04	-1.77	22.22	-1.39
V_{max}	Maximum N uptake rate	1.32	17.07	-1.25	22.46	-1.52
W/D	Wet / dry ratio	8.43	17.04	-1.26	22.36	-1.47
z	Culture depth	2	17.05	-1.26	21.64	-1.10
N_{min}	Minimum intracellular quota for N	10	20.85	0.69	17.51	1.02
<i>PON available at the IMTA site: effect baseline value is 12.32 tonnes</i>						
TGC	Thermal-unit growth coefficient*	2.33	15.49	2.57	9.59	2.22
FCR	Feed conversion	1.04	13.63	1.06	11.01	1.06

ratio*						
N_{content}	Nitrogen content in feed	0.07	13.59	1.03	11.05	1.03

1039

1040 * Time series variable. The time series parameters where increased/decreased by 10% at each
 1041 time step

1042 ** For the parameter “Nutrient state of seaweed at harvest” we used N_{min} instead of N_{max} at
 1043 the column labelled as +10% and $(N_{\text{min}} + N_{\text{max}})/2$ at the column labelled as -10%

1044